Answer to
Review of seNorge_2018, daily precipitation and temperature datasets over Norway by Cristian Lussana et al.

Dear Reviewer,

Thanks for your thoughtful and thorough work in revising our manuscript.

Point-by-point response to your review follows. The Reviewer's comments are reported in Italic.

Best Regards,
Cristian Lussana on behalf of the Authors

The authors have taken the pair of reviews and made substantive revisions to the manuscript that overall substantively improve readability of the piece as a whole. I have a number of queries and suggestions which should be considered prior to publication.

Major comments

1. At page 4 line 24-25 allusion is made to site exposures. A reader requires a reference to documentation of the site exposure method and further elucidation as to how, specifically, these were used.

Reply: page 4 line 24, the references for seNorge version 1.1 are reported (Mohr, 2008, 2009). The references include the definition of site exposure and its use for the production of seNorge 1.1.

2. The issue in p.7 line 4 over nomenclature persists. One of the Xi should be Xj surely and there should be a jth row or column?

Reply: the mathematical notation used is correct and consistent. In the paper by Sakov and Bertino (2011) pag. 227 first column, they define the notation that we have used. However, we have modified the text such that:

- **X** (bold capital X) indicates a matrix
- $\mathbf{X}_j$ (bold capital X with "j" as subscript) indicates the j-th column of matrix **X**
- $\mathbf{X}_{i,:}$ (bold capital X with "i,:" as subscript) indicates the i-th row of matrix **X**
- $\mathbf{X}_{ij}$ (bold capital X with "ij" as subscript) indicates the element at the i-th row and j-th column of matrix **X**

3. The example application for precipitation discussed in section 4 relates to vigorous large circulation cyclonic precipitation event which, naively, your method may perform best at. While it is understandable that you wish to show a high skill example it may also give a misleading impression. At a minimum this should be acknowledged. Ideally a more challenging situation such as a summer convective event should also be shown.

Reply: The objective of the example application is to illustrate the method used for the spatial analysis of precipitation. The selection of the case study (pag 11, lines 1-3) is based on the fact that for that specific day almost all the gauges have measured precipitation. This way, we thought the Figures would have been better suited for showing the step-by-step reconstruction of the precipitation field. We have not considered any measure of goodness-of-fit in the selection of the case study.

We avoid giving a misleading impression about the quality of the spatial analysis by verifying the performance of our method and discussing its pros and cons (Sections 5 and 6). In particular, for RR we have found

that the station density and the terrain complexity are the main factors determining the quality of our results, while the season of the year is a less important factor. These findings are in line with previous findings (e.g. Hofstra, 2008) and we have reported them in the paper (Discussion, page 16 lines 21-22; Conclusions, page 17 line 31).
For the reasons mentioned above, we believe that by adding another example application for precipitation we will not add significant information. An example of the performance of our method for a convective episode is reported in the following (see Section "Figures" below). At the beginning of August 2019 a thunderstorm occurred over Oslo (https://www.nrk.no/norge/se-hvordan-styrtregnet-splittet-oslo-1.14649700). This is an example of local-scale convective episode. Figure 4+ is equivalent to Figure 4 in the manuscript. Figure 5+ is equivalent to Figure 5 in the manuscript. Figure 6+ is equivalent to Figure 6 in the manuscript. The color scales are the same as in the manuscript. The key-messages one can extract from the Figures+ are rather similar to the ones that are described in the manuscript.

However, we think the Reviewer raises an interesting and important point. The readers may be interested in having a look at some precipitation (or temperature) fields before downloading the whole seNorge_2018 dataset. For this reason, we have included in the text some links to websites where it is possible to plot seNorge_2018 fields (see the Section "Code and data availability").

4. Why is the section 5.3 analysis limited to winter? Surely it would be valuable to show this for at least summer in addition, if not all seasons to build user confidence and understanding of the product strengths and limitations?

Reply: In the case of temperature, the occurrence of large errors as a function of station density for the summer season is discussed in Section 5.1.1 and shown in the bottom row of Fig. 7. Section 5.3 discuss more in detail the same issue but only for wintertime temperatures, such that the

limitations of our methods are emphasized. We have modified a bit the text to make this point clear to the reader.

In the case of precipitation, the verification shows that the season of the year is a less important factor than the station density (see the answer to Point 3). For this reason and in order to achieve more robust estimates, we have considered the whole dataset in Sec. 5.3.

We recognize there is a mistake in the text (page 15. Line 7). We have modified the text to correct the mistake.

5. Generally the figure captions are too short. Often text should be moved from the main body to the caption. The figure captions need to provide all information necessary for a reader to understand and interpret the figure and oftentimes this is missing.

Reply: we have revised all the figure captions.

Minor comments

1. Given the caveats rightly stated in the discussion the abstract at lines 11-12 on page 1 seems a bit unduly definitive?

Reply: In lines 11-12, two characteristics of the interpolation procedure are reported, such as: (i) the aggregated temperatures are interpolated separately (ii) physical consistency among them is enforced. Both statements are true.

2. P.3 line 21 described and discusses -> described and discussed

Reply: we have modified the text as suggested.

3. P.4 line 13 so to -> so as to

Reply: we have modified the text as suggested.

4. P.4 line 20 as precipitation -> as the precipitation

Reply: we have modified the text as suggested.

5. P.6 line 14 tend -> Tends?

Reply: we have modified the text “In the vicinity of an observation the IDI field is approximately equal to 1…”

6. Much of the paragraph starting p.6 line 28 should be moved to the figure caption rather than the text. Also: IDI equals to -> IDI equal to

Reply: we have modified the text as suggested.

7. I would provide a very brief synopsis of the section 6 discussion at p.7 line 15-16

Reply: The cross-checking is an important part and it is briefly summarized in the first paragraph of Sec. 3.1. We do believe that this paragraph is a brief synopsis of Sec. 6.

8. P.9 line 31 so to transform -> either to transform OR so as to transform

Reply: we have modified the text as suggested.

9. P.13 lines. 18-20 should be in an expanded figure caption instead of the main text.

Reply: we have modified the text to avoid repetition with the figure caption.

10. Please rephrase p.13 line 24 – it should not be about belief.

Reply: we have modified the text as suggested.

11. P.15 line 4 In this paragraph -> Next

Reply: we have modified the text as suggested.

12. Figure 3 caption projection of the differences is, I assume, an error, but I'm not sure what you actually intend to state here.

Reply: yes, it was an error. The caption has been corrected.

13. Figure 4 caption. Is the colour bar dimensionless units? If so state so. If not then give the units. Regardless please clarify the caption.

Reply: Yes, relative anomalies have dimensionless units and we have modified the caption to clarify it.

14. Figure 5 caption. Please help the reader out here. Are larger or smaller scales preferable? How does this scale partition between the methodological aspects and the event specific aspects? The event in question is a large cyclonic event which may have broad spatial scales. To what extent are the scales shown here a result of the event specific nature instead of the method? Intuitively the two must be intertwined and may be remedied by showing e.g. a summer convective event as suggested in major comments.

Reply: we have modified the caption of Figure 5 and extended in the text those parts describing the critical scale. In particular, we have discussed the points raised by the Reviewer.

15. Figure 8 caption should end: See Fig 7 caption for further details.

Reply: we have modified the text as suggested.

16. Figure 13 lower right panel RR -> RR DJF for consistency with remaining panels

Reply: This panel refers to RR and for this variable we have considered the whole dataset and not only the winter season (see also our answers to Major Comments 3 and 4). The figure caption has been modified to clarify this point.

Figures

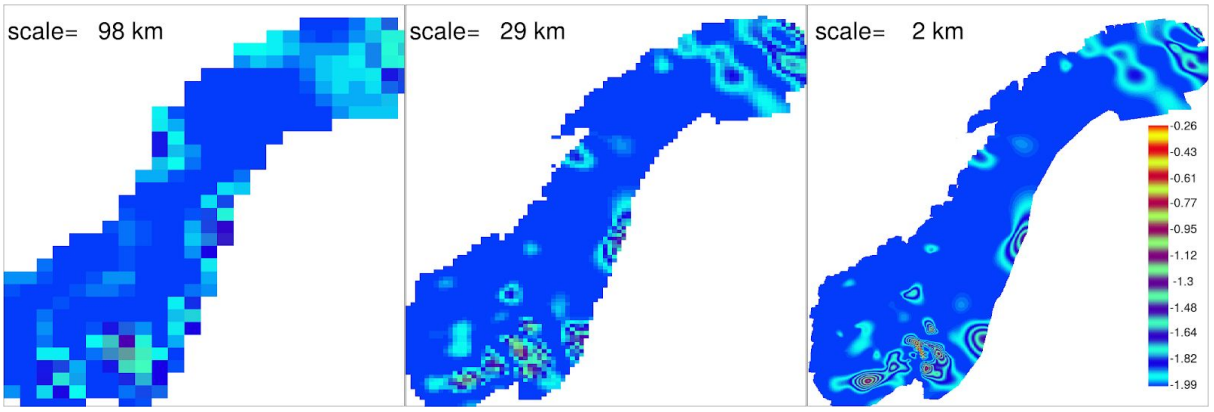

Figure 4+. 2019-08-04. See Figure 4 caption in the manuscript.

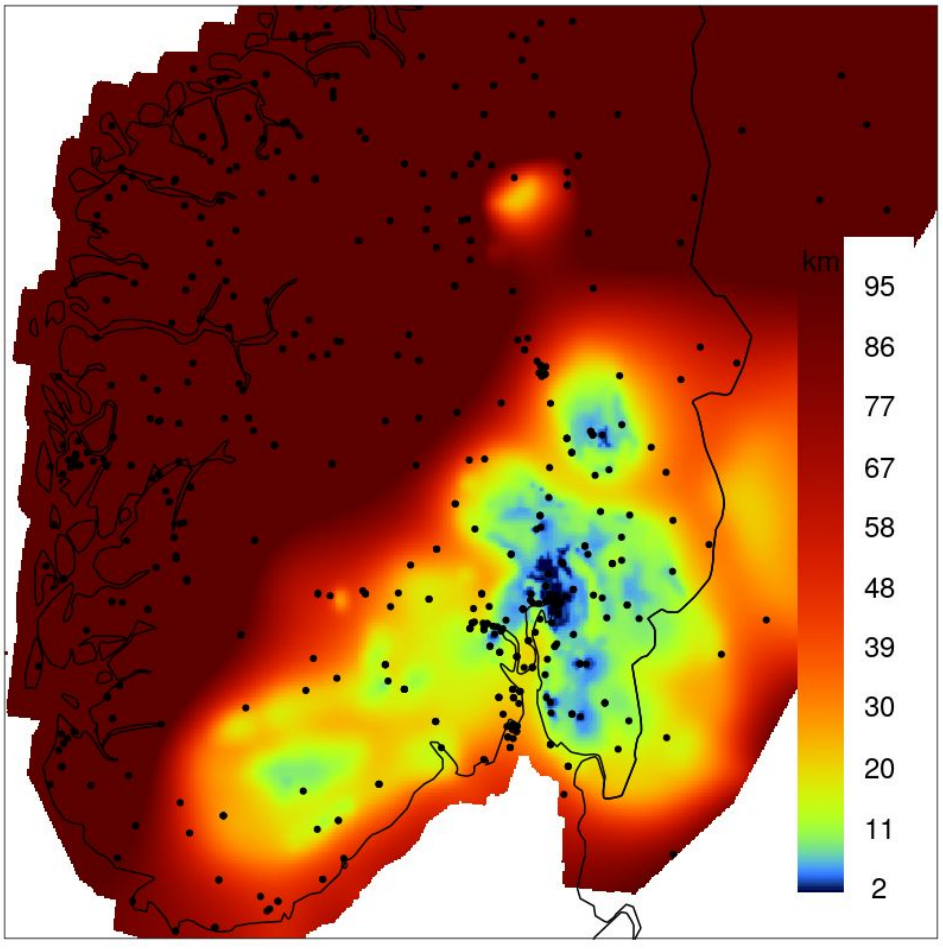

Figure 5+. 2019-08-04 RR. Critical scale. See Figure 5 caption in the manuscript.

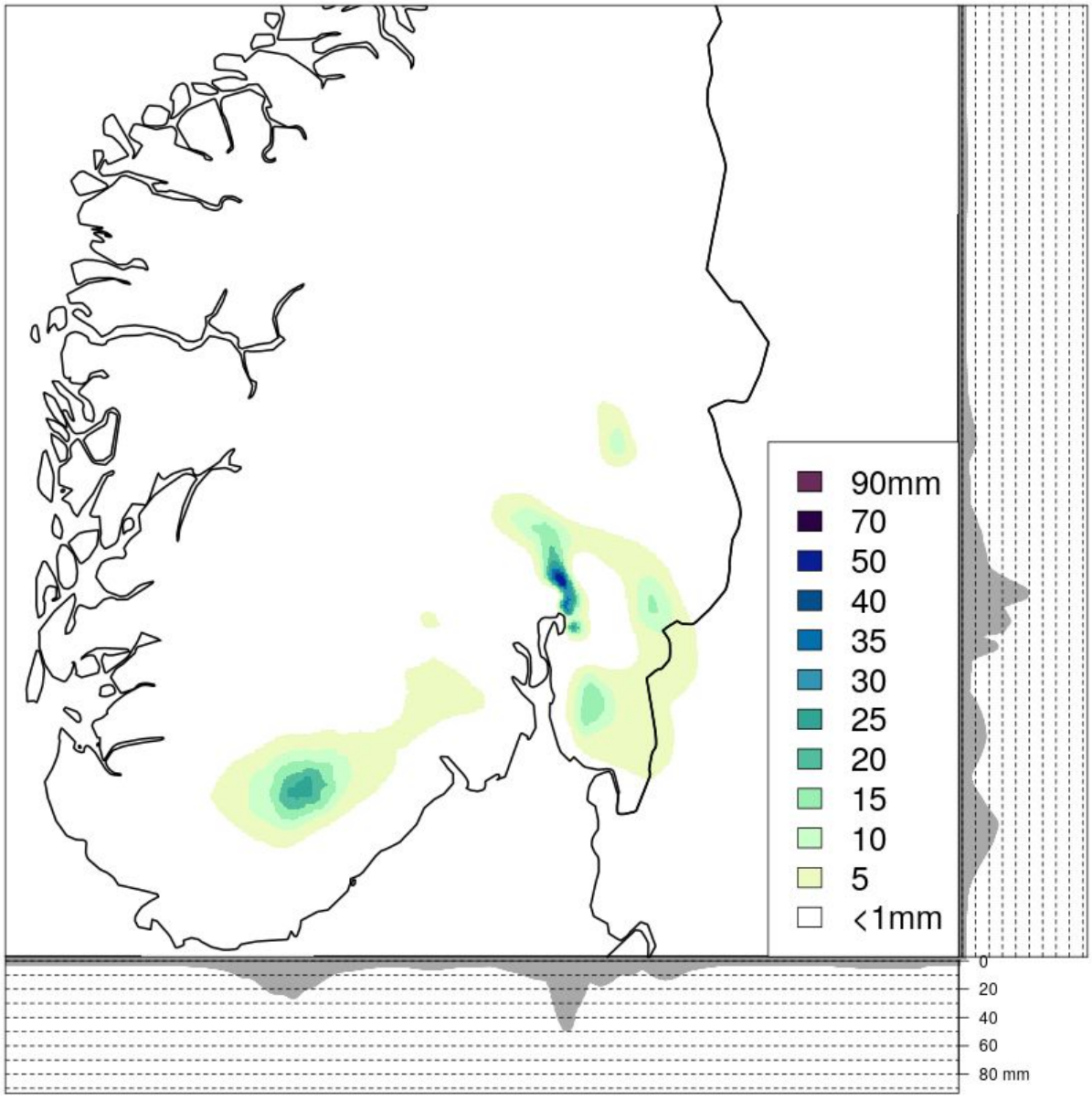

Figure 6+. 2019-08-04 RR analysis field. See Figure 6 caption in the manuscript.

seNorge_2018, daily precipitation and temperature datasets over Norway

Cristian Lussana[1], Ole Einar Tveito[1], Andreas Dobler[1], and Ketil Tunheim[1]

[1]Norwegian Meteorological Institute, Oslo, Norway

Correspondence: Cristian Lussana (critianl@met.no)

Abstract. seNorge_2018 is a collection of observational gridded datasets over Norway for: daily total precipitation; daily mean, maximum and minimum temperatures. The time period covers 1957 to 2017, and the data are presented over a high-resolution terrain-following grid with 1 km spacing in both meridional and zonal directions. The seNorge family of observational gridded datasets developed at the Norwegian Meteorological Institute (MET Norway) has a twenty-year long history and seNorge_2018 is its newest member, the first providing daily minimum and maximum temperatures. seNorge datasets are used for a wide range of applications in climatology, hydrology and meteorology. The observational dataset is based on MET Norway's climate data, which has been integrated by the "European Climate Assessment and Dataset" database. Two distinct statistical interpolation methods have been developed, one for temperature and the other for precipitation. They are both based on a spatial scale-separation approach where, at first, the analysis (i.e., predictions) at larger spatial scales are estimated. Subsequently they are used to infer the small-scale details down to a spatial scale comparable to the local observation density. Mean, maximum and minimum temperatures are interpolated separately, then physical consistency among them is enforced. For precipitation, in addition to observational data, the spatial interpolation makes use of information provided by a climate model. The analysis evaluation is based on cross-validation statistics and comparison with a previous seNorge version. The analysis quality is presented as a function of the local station density. We show that the occurrence of large errors in the analyses decays at an exponential rate with the increase in the station density. Temperature analyses over most of the domain are generally not affected by significant biases. However, during wintertime in data-sparse regions the analyzed minimum temperatures do have a bias between $2^{\circ}\mathrm{C}$ and $3^{\circ}\mathrm{C}$. Minimum temperatures are more challenging to represent and large errors are more frequent than for maximum and mean temperatures. The precipitation analysis quality depends crucially on station density: the frequency of occurrence of large errors for intense precipitation is less than 5% in data-dense regions, while it is approximately 30% in data-sparse regions. The open-access datasets are available for public download at: daily total precipitation (DOI:https://doi.org/10.5281/zenodo.2082320 **?**) ; daily mean (DOI:https://doi.org/10.5281/zenodo.2023997 **?**) , maximum (DOI:https://doi.org/10.5281/zenodo.2559372 **?**) and minimum (DOI:https://doi.org/10.5281/zenodo.2559354 **?**) temperatures

1 Introduction

Long-term observational gridded datasets of near-surface meteorological variables are widely used products. In climatology, they have been used for example to monitor the regional climate (**?**) and to validate and bias-correct climate simulations (**?**). In meteorology, they are used at national meteorological institutes, such as the Norwegian Meteorological Institute (MET Norway), to monitor and report the weather conditions. In hydrology, they are used as external forcing for hydrological and snow modeling (**???**).

seNorge_2018 is a collection of four long-term observational datasets over Norway covering the 61-year time period 1957-2017 for: daily total precipitation (RR), daily mean temperature (TG), daily minimum (TN) and maximum (TX) temperatures. It builds upon the previous work on establishing MET Norway's observational datasets (**???**) and the core of its statistical interpolation method is the Optimal Interpolation (OI, **??**). A review of the relevant literature for our spatial interpolation applications is given in the paper by **?**.

Like the previous versions of seNorge, precipitation and temperature data are provided on a high-resolution grid with 1 km grid spacing in both meridional and zonal directions. seNorge_2018 aims at achieving a higher effective resolution of the analyzed (or predicted) fields than the previous versions. It is worth spending a few words on effective resolution in OI. The difference between grid spacing and resolution is described by **?**. In the context of numerical modeling, **?** defines the effective resolution as "the minimum wavelength the model can describe with some required level of accuracy (not defined)" and it concludes that as many as 10 gridpoints may be required to properly represent a field. As pointed out by **?**, there is a subjective component in the number of gridpoints needed to resolve a feature in a field. In contrast to in-situ observations which represent point values, our gridded analyses produce areal averages. What this means is that for each grid point, we calculate weighted averages of the nearest observations. The larger the extensions of the spatial supports for these averages, the lower the effective resolution of the analysis fields. In short, it is the availability of measurements that determines the highest possible effective resolution, irrespective of the chosen grid spacing, with topographic complexity a compounding factor (**?**). The settings used in the interpolation must consider this limitation, and if the same settings are to be used over the whole area, then the sub-region of lowest station density may dictate the effective resolution of the entire domain.

The following definitions of spatial scales are used in the text. Regional scale coincides with the whole domain. Given the importance of the observational network, at an arbitrary point we refer to scales that are defined with respect to the station distribution in its surroundings. Sub-regional scale (or local scale) defines an area -around the point- that includes dozens of observations (10-100). Small-scale defines an area that includes few observations (1-10). Unresolved scale refers to those spatial scales that are smaller than the average distance between a station and its closest neighbours, such that atmospheric fields could not be properly represented by the observational network.

The main original aspect of our research is that the spatial interpolation methods automatically adapt OI settings to the local station density, such that in data-dense regions the spatial supports of the areal-averaged analyses are smaller than in data-sparse regions. In other words, the effective resolution of the analysis fields is higher in data-dense than in data-sparse regions.

Because the spatial analysis depends on station density, the Integral Data Influence (IDI: **??**) has been used as a diagnostic parameter to quantify the effects of station density on the analysis.

The presented research includes several other original aspects. In the case of precipitation, the measurements have been adjusted for the wind-induced under-catch in a way that is consistent with the method proposed by **?**. A multi-scale OI scheme has been implemented on precipitation relative anomalies with respect to a reference field that captures the field variability at unresolved spatial scales. The reference fields are the monthly totals derived from a regional climate simulation with a resolution of 2.5 km. The climate simulation is based on the dynamical downscaling of the global reanalysis ERAInterim and it is available for the time period 2003-2016. In the paper by **?**, it has been demonstrated that the combination of the same model fields with observed data do improve the representation of monthly total precipitation over Norway. **?** proved that the use of a reference field as a first guess for the precipitation patterns is a successful approach also in the Alps. They found that daily precipitation over the Alpine region is well represented by using the seasonal precipitation mean as a single predictor field in Kriging with external drift.

In the case of temperature, seNorge_2018 is the first seNorge dataset that includes daily minimum and maximum temperatures. The availability of these two additional variables allow for the computation of several more indices for climate variability and extremes, such as the ones reported in the paper by **?**. The three temperature variables are treated separately with the same interpolation method. With respect to seNorge2 (**?**), the regional spatial trend of temperature is obtained as the blending of a much larger number of sub-regional trends. The analysis method has been implemented on a gridpoint-by-gridpoint basis in order to take advantage of a local Kalman gain.

The structure of the paper is as follows. Section

2 Data

2.1 Observations

The in-situ observations are retrieved from MET Norway's climate database and the European Climate Assessment and Dataset (ECA&D, **?**). The spatial domain covers the Norwegian mainland, plus an adjacent strip of land extending into Sweden, Finland and Russia in order to reduce boundary effects along the Norwegian border. The observations have been quality controlled by experienced staff and with the help of automatic procedures, such as the spatial consistency test described by **?**. The variables are defined as following: TG is the 24-hour average between 06:00 UTC of the day, reported as time-stamp and 06:00 UTC of the previous day; RR is the accumulated precipitation over the same time interval as TG, moreover RR data has been corrected for the wind-induced under-catch of the gauges; TX and TN are, respectively, the maximum and minimum observed temperatures between 18:00 UTC of the day reported as time-stamp and 18:00 UTC of the previous day. TG and RR share the same day-definition so as to serve hydrological applications (**??**). As a result of choices made in the past at MET Norway, TX and TN have a different day definition than RR and TG.

The measured RR value (i.e., RR_{raw}) at an arbitrary location is adjusted for wind-induced under-catch of solid precipitation by means of a procedure similar to the one presented by **?**:

$$\alpha = \tau_1 + (\tau_2 - \tau_1)\left\{\exp\left[(\mathrm{TG} - T_\tau)/s_\tau\right]/\left(1 + \exp\left[(\mathrm{TG} - T_\tau)/s_\tau\right]\right)\right\} \quad (1)$$

$$\gamma = [1-\alpha]\exp\left[-(W/\theta)^\beta\right] + \alpha \quad (2)$$

$$\mathrm{RR} = \gamma^{-1}\,\mathrm{RR}_{raw} \quad (3)$$

where TG is extracted from the analysis field (Sec.

Figure

2.2 Reference fields for spatial interpolation of precipitation

The reference fields are derived from long-term averages calculated from the output of a high-resolution numerical model. The reference datasets used for precipitation are based on hourly precipitation provided by the climate model version of HARMONIE (version cy38h1.2), a seamless NWP model framework developed and used by several national meteorological services. HARMONIE includes a set of different physics packages adapted for different horizontal resolutions. For the high-resolution, convection permitting simulations in this case, the model has been set-up with AROME physics (**?**) and the SURFEX surface scheme (**?**). The climate runs have been carried out within the HARMONIE script system, covering the period July 2003 to December 2016 on a 2.5 km grid over the Norwegian mainland. More details on the climate model can be found in **?**, references therein and on https://www.hirlam.org/trac/wiki/HarmonieClimate. The numerical model does not include measurements from the network of rain-gauges. The mean monthly total precipitation fields have been computed considering the available hourly data and they have been used as reference fields for the spatial interpolation of precipitation as described in Sec.

Over our domain, we have chosen not to use precipitation climatologies derived by observational gridded datasets as the reference because in some regions the observational network is extremely sparse (Fig.

2.3 Integral Data Influence

IDI is similar to the degrees of freedom introduced by **?** and it has been used also to evaluate the distribution of weather stations (**?**). In practice, IDI is obtained as the result of an OI performed by arbitrarily assigning a value of 1 to the observations (i.e., maximum amount of available information) and the reference value of 0 to the background (i.e, basic amount of information available everywhere). The analytical function that usually represents the background error correlation in OI, in the case of IDI is representing the station influence on the analysis according to a predefined metric. This metric is defined as a function of the geographical parameters. For an arbitrary point in space, the geographical parameters are stored in a vector $\mathbf{r}$ having four components: latitude, longitude, altitude and land area fraction (i.e. fraction of land in the 1 km square box centered at the point). The land area fraction is introduced here and used in Sec.

For the purpose of evaluation in Sec.

In the two maps of Fig.

For temperature, elevation plays a predominant role and even only a few stations at higher elevations can provide a reasonable approximation of the sub-regional near-surface temperature lapse rate. Fig.

For precipitation, the IDI map in Fig.

Fig.

3 Spatial Interpolation methods

The notation used is based on both **?** and **?**. The number of gridpoints is m. The number of observations is p. Upper-case bold symbols are used for matrices, lower-case bold symbols for vectors and italic symbols for scalars. For an arbitrary matrix $\mathbf{X}$, [..[1]]$\mathbf{X}_j$ means the jth column; $\mathbf{X}_{i,:}$ the ith row; and $\mathbf{X}_{ij}$ the element at the ith row and jth column. For an arbitrary vector $\mathbf{x}$, $\mathbf{x}_i$ denotes the ith element. The superscripts on the upper left hand corner of a symbol identify: analysis a; background b; observation o. Upper accents have been used too. In the case of temperature, where we iterate over the gridpoints, the notation $\overset{i}{\mathbf{X}}$ indicates that matrix $\mathbf{X}$ is valid for the ith gridpoint and in this sense we may refer to it as a local matrix. In the case of precipitation, where we iterate over spatial scales, those length scales are indicated with greek letters and the notation $\overset{\alpha}{\mathbf{X}}$ indicates that matrix $\mathbf{X}$ is obtained as a function of the spatial scale of α km. Upper accents are not used only for matrices, for instance the in-situ observations are stored in the p-vector $\mathbf{y}^o$ but in the following we will refer to the $\overset{i}{p}$-vector $\overset{i}{\mathbf{y}}^o$ of the nearest observations to the ith gridpoint.

3.1 Statistical interpolation of temperature

The same interpolation scheme is used for the mean, the maximum and the minimum daily temperature. The physical consistency among the three variables is assured by post-processing the independently analyzed datasets and for each gridpoint we impose that: TN is always smaller or equal to TG; TX is always greater or equal to TG. The cross-checking is further discussed in Sec. [..[2]]

.

The spatial interpolation is implemented on a gridpoint-by-gridpoint basis. It combines a regional pseudo-background field, that is the weighted average of numerous sub-regional fields, with the observations. The temperature analysis at the generic ith gridpoint is written as:

$$\mathbf{x}_i^a = \mathbf{x}_i^b + \overset{i}{\mathbf{K}}_{i,:} \left(\overset{i}{\mathbf{y}}^o - \overset{i}{\mathbf{y}}^b \right) \tag{4}$$

$\overset{i}{\mathbf{y}}^o$ and $\overset{i}{\mathbf{y}}^b$ are $\overset{i}{p}$-vectors of the nearest stations to the ith gridpoint.

The local Kalman gain in Eq. (is:

$$\overset{i}{\mathbf{K}}_{i,:} = \overset{i}{\mathbf{G}}_{i,:} \left(\overset{i}{\mathbf{S}} + \varepsilon^2 \overset{i}{\mathbf{I}} \right)^{-1} \tag{5}$$

[1] removed: $\mathbf{X}_i$ means the i

[2] removed:

$\overset{i}{\mathbf{I}}$ is the $\overset{i}{p}$x$\overset{i}{p}$ identity matrix and $\varepsilon^2 \equiv \sigma_o^2/\sigma_b^2$ is the ratio between the constant observed (σ_o^2) and pseudo-background (σ_b^2) error variances that has been set to 0.5, as for seNorge2 (**?**). The local pseudo-background error correlation matrices are defined on the basis of the correlation function between pair of points $\rho^T(\mathbf{r}_j, \mathbf{r}_k)$ as:

$$\rho^T(\mathbf{r}_j, \mathbf{r}_k) = f_d\left(\mathbf{r}_j, \mathbf{r}_k; D_i^h\right) \;\; f_z\left(\mathbf{r}_j, \mathbf{r}_k; D^z\right) \;\; [1 - (1 - w_{min})|w(\mathbf{r}_j, \mathbf{r}_k)|] \tag{6}$$

such that the correlation between the jth gridpoint and the kth station is $\overset{i}{\mathbf{G}}_{jk} = \rho^T(\mathbf{r}_j, \mathbf{r}_k)$. Analogously, the correlation between the jth station and the kth station is $\overset{i}{\mathbf{S}}_{jk} = \rho^T(\mathbf{r}_j, \mathbf{r}_k)$. The Gaussian functions f are defined in Eq. (. A formulation similar to Eq. (has been used in the paper by **?**, in that case the land area fraction has been replaced by the land use. w_{min} sets the minimum value for the factor related to land area fraction when $w(\mathbf{r}_i, \mathbf{r}_j)$ is maximum (i.e., equals to 1). D^z and w_{min} are fixed over the domain, while D_i^h is allowed to vary between gridpoints, although with some restrictions. In an ideal situation of a very dense observational network, one may consider to rely on adaptive estimates for the three parameters. This is not the case for our station distribution, so we have opted for a "hybrid" configuration (i.e., D^z and w_{min} fixed; D^h adaptive) that would return robust estimates. The impact of large land area fraction differences on ρ^T is less dramatic than those of large horizontal or elevation differences and it also impacts only a limited number of stations along the coast. Eventually, we have manually set $w_{min} = 0.5$ to achieve the desired effect of attenuating the influence of coastal areas over inland areas and vice versa, while at the same time avoiding the introduction of sharp gradients between those two regions. The optimization procedure for D_i^h and D^z is described in the following of this section.

The pseudo-background x_i^b in Eq. (is the blending of n sub-regional pseudo-backgrounds and it is in many ways similar to those described by **?**. Each sub-regional pseudo-background is defined by a centroid and it includes only the 30 stations closest to this centroid. The pseudo-background field with centroid at $\mathbf{r}_c$ is the m-vector $\overset{c}{\mathbf{x}}^b$ and its value at the ith gridpoint is $\overset{c}{\mathbf{x}}_i^b$. The seNorge_2018 domain has been divided on a 50x50 grid, each cell is a 24 km by 31 km rectangular box and the nodes (i.e., centres of the cells) are the "candidate" centroids. If a node is inside the domain and has at least 30 stations in a neighbourhood of 250 km, then it is a suitable centroid. Those 30 temperature observations are used to estimate a sub-regional pseudo-background field as a function of the elevation only. The analytical function used to model the vertical profile of temperature is the one proposed by **?** for the alpine region and its parameters have been obtained by fitting the function to the aforementioned 30 observations. We assume that 30 observations can provide a reliable fitting. The generic cth pseudo-background field $\overset{c}{\mathbf{x}}^b$ is derived directly from the digital elevation model by assuming that the cth sub-regional vertical temperature profile is valid for the whole domain. By using a 50x50 grid, the number of sub-regions n is usually between 500 and 600 and there are significant overlaps between neighbouring sub-regions, such that the continuity of the regional pseudo-background is guaranteed. Finally, $\mathbf{x}_i^b$ is a weighted average of n values:

$$\mathbf{x}_i^b = \frac{\sum_{c=1}^{n} \overset{c}{\mathbf{x}}_i^w \, \overset{c}{\mathbf{x}}_i^b}{\sum_{c=1}^{n} \overset{c}{\mathbf{x}}_i^w} \tag{7}$$

where the weights at the ith gridpoint $\overset{c}{\mathbf{x}}_i^w$ are the n IDI values (Sec.

The optimization of D^z and D_i^h of Eq. (is based on the statistics of the innovation (i.e. observation minus background) at station locations. As described by **?**, the elements of the background error covariance matrix at station locations, which is modeled by us as $\sigma_b^2\mathbf{S}$, should match the innovation sample covariances. In Tables

3.2 Statistical interpolation of precipitation

The multi-scale OI analyses are the results of successive approximations of the observations over a sequence of decreasing spatial scales that at station locations converge to the observed values.

The interpolation scheme is not applied directly to the RR values (the vector of the raw observed values adjusted for the wind-induced under-catch is indicated as $\mathbf{y}^{\mathrm{rr}}$) but to their anomalies relative to a reference field of monthly precipitation (see Sec.

The analysis procedure can be written as:

$$\mathbf{x}^a = g^{-1}\left[\mathcal{M}_2 \circ \mathcal{M}_3 \circ \ldots \circ \mathcal{M}_\eta\left(\tilde{\mathbf{x}}^a\right)\right] \odot \mathbf{x}^{\mathrm{ref}} \tag{8}$$

where the three fundamental operations are: (1) the composition of several applications of the same statistical interpolation model down a hierarchy of spatial scales of $\{\eta\,\mathrm{km}, \ldots, 3\,\mathrm{km}, 2\,\mathrm{km}\}$, such that the results of a model application are used to initialize the successive one, $\circ$ stands for model composition and $\mathcal{M}_\eta$ stands for the application of the statistical model to the largest length scale of η km, $\tilde{\mathbf{x}}^a$ is the average of the $\mathbf{y}^o$ elements; (2) the Box-Cox inverse-transformation $g^{-1}()$; (3) the elementwise multiplication of vectors $\odot$ [..[3]]to transform the relative anomalies into RR values and at the same time include the effects of unresolved spatial scales. Ideally, the sequence of spatial scales to be used in Eq. (should be bounded between a very large scale (e.g, half the largest domain dimension) and a fine scale corresponding to the average distance between two stations in data-dense areas. The number of scales in between those two extremes is not critical for the final results, provided that they are enough to guarantee a continuous analysis field in all situations. For seNorge_2018, we are using approximately 100 scales with a minimum of 2 km and a maximum of 1400 km. According to **??**, those spatial scales range from the regional synoptic down to the lower boundary of the mesoscale. The sequence is unevenly spaced as the difference between two consecutive scales is somewhat proportional to their values.

The step-by-step description of the model $\overset{\alpha}{\mathbf{x}}{}^a = \mathcal{M}_\alpha\left(\overset{\beta}{\mathbf{x}}{}^a\right)$ for two [..[4]]arbitrary consecutive length scales of β km and α km (with $\beta > \alpha$) is:

$$\overset{\alpha}{\mathbf{x}}{}^b = \overset{\alpha}{\mathbf{\Psi}}\overset{\beta}{\mathbf{x}}{}^a \tag{9}$$

$$\overset{\alpha}{\mathbf{K}} = \overset{\alpha}{\mathbf{G}}\left(\overset{\alpha}{\mathbf{S}} + \varepsilon^2\overset{\alpha}{\mathbf{I}}\right)^{-1} \tag{10}$$

$$\overset{\alpha}{\mathbf{x}}{}^a = \overset{\alpha}{\mathbf{x}}{}^b + \overset{\alpha}{\mathbf{K}}\left(\mathbf{y}^o - \overset{\alpha}{\mathbf{H}}\overset{\alpha}{\mathbf{x}}{}^b\right) \tag{11}$$

In order to reduce the multi-scale OI computational expenses, the original 1 km grid is aggregated onto a new coarser grid, with aggregation factor equal to the integer value nearest to $(\alpha/2)$ km. The aggregation groups several smaller rectangular boxes

[3] removed: so

[4] removed: successive and arbitrary

into a bigger one (e.g., if $\alpha = 8$ km then 16 of the 1 km by 1 km boxes are aggregated into a single box measuring 4 km by 4 km). The analysis at scale β is used as the background for scale α in an OI scheme. The analysis values are transferred between the two non-matching grid by the operator $\overset{\alpha}{\mathbf{\Psi}}$ of Eq. (, that is a bilinear interpolation mapping vectors on the (coarser) β-grid to vectors on the (finer) α-grid. The observation operator $\overset{\alpha}{\mathbf{H}}$ of Eq. (is also a bilinear interpolation transforming vectors on the α-grid to p-vectors. ε^2 is set 1, which means that observations and background are assumed the have the same error variances. The background error correlation matrices of Eq. (are defined on the basis of the correlation function ρ^R:

$$\rho^R(\mathbf{r}_j, \mathbf{r}_k) = f_d(\mathbf{r}_j, \mathbf{r}_k; \alpha) \tag{12}$$

The Gaussian function f is defined in Eq. (and the notation is similar to Eq. (. Note that the length scales enter multi-scale OI of Eq. (through the correlation function of Eq. (.

An OI scheme such as the one presented in Eq. (- (is realizing a low-pass filter whose cut-off wavelength is approximately α km (**?**) so every iteration over a smaller spatial scale returns a field with more fine-scale details in it. For a given element of the observation vector, there may be a [..[5]]*critical* scale at which the background coincides exactly with the observed value such that its contribution to the innovation in Eq. ((i.e., the term in parentheses) is equal to zero[..[6]]. As a consequence, the analysis values $\overset{\alpha}{\mathbf{x}}^a$ in the surroundings of that observation are unlikely to change in the passage between scales α and β and those analysis values are also unlikely to change over the subsequent iterations [..[7]]because all the available information has been yet used by the interpolation scheme. For the ith gridpoint, the critical scale can be defined as the spatial scale α where the last significant variation of the interpolated relative anomaly $\overset{\alpha}{\mathbf{x}}{}^a{}_i$ has occurred with respect to the value $\overset{\beta}{\mathbf{x}}{}^a{}_i$ (or equivalently $\overset{\alpha}{\mathbf{x}}{}^b{}_i$) obtained for the immediately preceding scale β. The critical scale is variable across the domain and depends on both the spatial structure of the precipitation field and the local station density. The smaller the critical scale, the more noisy and rough is the analysis field. Typically, stratiform precipitation would lead to larger critical scales than convective precipitation. In any case, the small-scales determined locally by the observational network, as defined in the Introduction, pose lower limits to the critical scale.

4 Example application for precipitation

An example of application of the spatial interpolation method described in Sec.

The reference field for October (see Sec.

The first of the three fundamental steps in Eq. (is the iterative application of OI for the Box-Cox transformed relative anomalies over a sequence of decreasing spatial scales. We are looping over 91 scales and in Fig.

Figure

Fig.

[5] removed: "critical"

[6] removed: and its analysis value would not

[7] removed: . That

5 Verification

The evaluation is based mostly on CV exercises and comparison against the seNorge2 datasets of RR and TG. The cross-validation analysis (i.e., CV-analysis) is the analysis value at a station location obtained considering a selection of the available observations that does not include the one measured at that location. If CV is applied systematically to all stations and it includes all the remaining observations then it is called leave-one-out cross-validation (LOOCV).

The summary statistics of the following variables are used: CV-analysis residuals (i.e, CV-analyses minus observations); innovations (i.e., background minus observations); and analysis residuals (i.e, analyses minus background). The CV-analysis, background and analysis are evaluated through the statistics of CV-analysis residuals, innovations and analysis residuals, respectively. Note that the background is not considered in the verification of precipitation. At a generic station location, CV-analysis and background are independent from the observation, while the analysis has been computed using the observation. As a consequence, the statistics of CV-analysis residuals and innovations have similar interpretations. The CV-analysis residual distributions are used in place of the unknown analysis error distributions at gridpoints. The innovation distributions are used to investigate the properties of the background error at gridpoints. On the other hand, the statistics of analysis residuals reveal the filtering properties of the statistical interpolation at station locations that are related to the observation representativeness error (**???**). The mean absolute error (MAE) and the root mean square error (RMSE) quantify the average mean absolute deviation and the spread, respectively, of a variable.

For temperature, we are using LOOCV. The comparison between the statistics of CV-analysis residuals and innovations quantifies the improvement of the analysis over the pseudo-background at gridpoints. The fraction of errors (i.e., absolute deviations) greater than 3°C has been used as a measure of the tails of the distribution of deviation values. Note that the threshold of 3°C is used in MET Norway's verification practice to define a significant deviation that undermines the user's confidence in the forecast.

For precipitation, LOOCV is computationally too expensive. Thus, for each day a random sample of 10% of the available stations have been reserved for CV and they are not used in the interpolation. Because precipitation errors follow a multiplicative rather than an additive error model (**?**), large errors for precipitation are defined as absolute deviations between CV-analysis and observation greater than 50% of the observed value.

5.1 Temperature

5.1.1 Summary statistics of the verification scores at station locations

In Figures

For all variables, the spatial interpolation scheme generally performs better during summer than winter when small-scale processes (e.g., strong temperature inversion) are more frequent. The TG analysis error distribution at gridpoints, as estimated by CV-analysis residuals, shows that during the summer, the MAE is between 0.5°C and 1°C and its RMSE is also around 1°C, and errors larger than 3°C are unlikely even in data-sparse regions; during winter, MAE and RMSE double their values and the differences between data-dense and data-sparse regions are larger, with the probability of having large errors being

approximately 25% in data-sparse regions. The TX analysis error behaves similarly to TG. Note that the spatial interpolation method during summer performs better on TG than on TX, while in winter the opposite occurs. The distribution of the TN analysis error at gridpoints has a much larger spread than those of TG and TX. The TN RMSE is between 1.5°C and 2°C in summer, and up to approximately 4°C during winter in data-sparse regions. The tail of the TN distribution is also longer and large errors are more frequent than for the other daily temperatures. At the same time, the average bias (MAE) is also larger for TN.

5.1.2 seNorge_2018 and seNorge2 comparison of TG

The seNorge_2018 spatial interpolation procedure builds upon seNorge2. Several modifications have been made, though keeping the scale-separation approach. In seNorge_2018 a single function has been used to model the sub-regional vertical profile, instead of the three different functions used in seNorge2. At the same time, in seNorge_2018 the blending of sub-regional fields into a regional pseudo-background field is based on a much larger number of sub-regional fields.

In Figure

[..[8]]The variations between seNorge_2018 and seNorge2 having the most significant impacts on the differences shown in Fig.

The evident differences between the two datasets are in the mountains, where seNorge_2018 often presents warmer valley floors and colder ridges. In particular, according to Fig.

5.2 Precipitation

5.2.1 Summary statistics of the verification scores

In Figure

The close relationship between the terrain and the annual total precipitation is shown in Fig.

5.2.2 seNorge_2018 and seNorge2 comparison

Figure

For precipitation, we have stated in the Introduction that seNorge_2018 uses a reference to increase the effective resolution of the field, compared to the resolution given by the spatial distribution of the observational network alone. In the context of forecast verification, **?** decompose precipitation fields on different spatial scales using a two-dimensional discrete Haar wavelet decomposition. As described in the paper by **?**, this wavelet decomposition can be used to study the average energy per cell (hereafter energy) of the scale components of precipitation, where the energy is defined as ”the average of the field gridpoint squared value”. Fig.

[8] removed: We believe that the

5.3 Occurrence of large errors as a function of the station density

[..[9]]Next we discuss more in detail the relationships between the occurrence of large errors, as they have been defined at the beginning of Sec.

In Figure

As for temperature, the expected percentage of large errors over the precipitation grid is shown in Fig.

6 Discussion

Because the presented statistical interpolation methods automatically adapt to the local observation density, the user of the seNorge_2018 dataset must be aware that: (i) the comparison between different sub-regions over the domain is influenced by the respective local station densities, and (ii) variations in the observational network over time will affect temporal trends derived from this dataset (**?**).

For the four variables, we have investigated the variations of the performances of our interpolation schemes between two different time periods, 1961-1990 (61-90) and 1991-2015 (91-15). The evaluation scores are similar to the ones presented in Sec.

The three main factors determining the quality of the temperature datasets are the season of the year, the station density and the terrain complexity. The last two factors are correlated, as shown by Figs.

The two main factors determining the quality of the precipitation dataset are the station density and the terrain complexity. The season of the year seems to have a smaller impact on the verification scores.

With respect to seNorge2, seNorge_2018 presents several methodological improvements and two additional variables, TX and TN. Furthermore, it should be mentioned that there had been variations in the observational datasets used for the production of the two gridded datasets. Even though the data sources are the same for both seNorge datasets, seNorge2 is based on an observational dataset that has been produced in 2016, while seNorge_2018 benefits from the latest efforts in data collection and quality control made by MET and the ECA&D team. The verification results show that seNorge_2018 temperature predictions are on average more accurate than seNorge2, especially along the coast. With respect to the predictions of precipitation, as described in the seNorge2 paper **?**, this dataset is likely to underestimate precipitation so we have designed seNorge_2018 to returns higher precipitation values because this would better agree with the Norwegian water balance and eventually improve the results of hydrological simulations based on seNorge_2018 than for seNorge2. This last point needs to be verified in the near future. In Sec.

6.1 TG, TX and TN cross-checking

The cross-checking is mentioned at the beginning of Sec.

[9] removed: In this paragraph

Because of the 12-hour offset in the definitions of TG and either TX or TN, the cross-checking can be wrong. Nevertheless, it is a useful check to identify those situations where the interpolation of daily extremes is not convincing. In fact, despite the offset in the definitions of the 24-hour aggregation period, for a typical day TN is smaller than TG and TX is greater than TG. We have found very rare exceptions to these rules in the surroundings of station locations. In the vast majority of cases, the cross-checking flags those gridpoints in the mountains (i.e., far from station locations) where the extrapolation of the vertical profile cannot be adjusted by means of observed data, which are located in large part on the valley floors (Fig.

The number of gridpoints flagged by the cross-checking vary seasonally and it is higher in winter and lower in summer. In the case of TN, the cross-checking flags on average 9% of the gridpoints in winter and 1% in summer. In the case of TX, the cross-checking flags on average 7% of the gridpoints in winter and 1% in summer.

Future developments will focus on improving the cross-checking, in order to properly handle those exceptional situations that are currently erroneously flagged as physical inconsistencies among the three variables.

7 Conclusions

seNorge_2018 provides 61-year (1957-2017) datasets of daily mean, maximum, and minimum temperatures, as well as daily total precipitation, over Norway and parts of Finland, Sweden and Russia. The plan at MET Norway is to update the historical dataset once a year, while at the same time provisional daily estimates for the current year are computed every day. MET Norway has an open data policy and all the datasets, as well as most of the observations used in the calculations, are available for public download via its web services.

The observational datasets have been obtained through statistical methods that build upon our previous works. The interpolation schemes automatically adapt their settings to the local station density and this allows for a higher effective resolution in data-dense areas, while in data-sparse regions the analysis is always the estimate of at least a few stations.

The main factor determining the quality of the temperature analysis are: the season of the year, the station density and the terrain complexity. In the case of precipitation, those factors are: the station density and the terrain complexity. Because of the importance of the combination of station density and terrain, we have widely used the IDI concept in our evaluation.

The new seNorge_2018 shows significant differences when compared to its predecessor seNorge2, both for TG and especially for RR. While first qualitative evaluations indicate that this is an improvement, an indirect evaluation where seNorge_2018 would be used as the forcing data for snow- and hydrological modeling is needed to confirm this.

seNorge_2018 is MET Norway's first observational dataset providing TX and TN from 1957. The temperature analysis has the largest errors during winter and the TN is the most challenging variable to represent. For TG and TX, large analysis errors are expected only in winter and limited to almost data-void areas such as mountain tops. TN may present large analysis errors more often than TG and TX and for larger portions of the domain, especially in mountainous regions.

To fill commonly occurring spatial gaps for RR in data-sparse regions, the interpolation uses monthly fields of a high-resolution numerical model and adjusts this to an optimal fit with the measurements that are available in the area. As a result, seNorge_2018 has a finer effective resolution than seNorge2. The ability of the method to correctly distinguish between pre-

cipitation and no-precipitation depends critically on the station density. In the North, the sparser observational network is associated with a high occurrence of large analysis errors. The evaluation shows that large analysis errors are unlikely in the data-dense regions of Southern Norway, even for intense precipitation.

8 Code and data availability

The spatial interpolation software is available at (DOI:https://doi.org/10.5281/zenodo.2022479, **?**).

The open-access datasets are available for public download at:

- daily total precipitation (DOI:https://doi.org/10.5281/zenodo.2082320, **?**)
- daily mean temperature (DOI:https://doi.org/10.5281/zenodo.2023997, **?**)
- daily maximum temperature (DOI:https://doi.org/10.5281/zenodo.2559372, **?**)
- daily minimum temperature (DOI:https://doi.org/10.5281/zenodo.2559354, **?**)

seNorge_2018 is daily updated by MET Norway and the most recent data are available at http://thredds.met.no/thredds/catalog/senorge/seNorge_2018/catalog.html. Furthermore, it is possible to access the maps of precipitation or temperature analyses via:

- xgeo.no. Select *All Data* from the main menu, then *Weather*, then *seNorge_2018 precipitation* or *seNorge_2018 temperature*.
- http://thredds.met.no/thredds/catalog/senorge/seNorge_2018/catalog.html. Select a file (e.g., Latest/seNorge2018_20190815.nc), then *Viewers* and *Godiva2*.

Acknowledgements. This research has been partially funded by the Norwegian project "Felles aktiviteter NVE-MET tilknyttet nasjonal flom- og skredvarslingstjeneste".

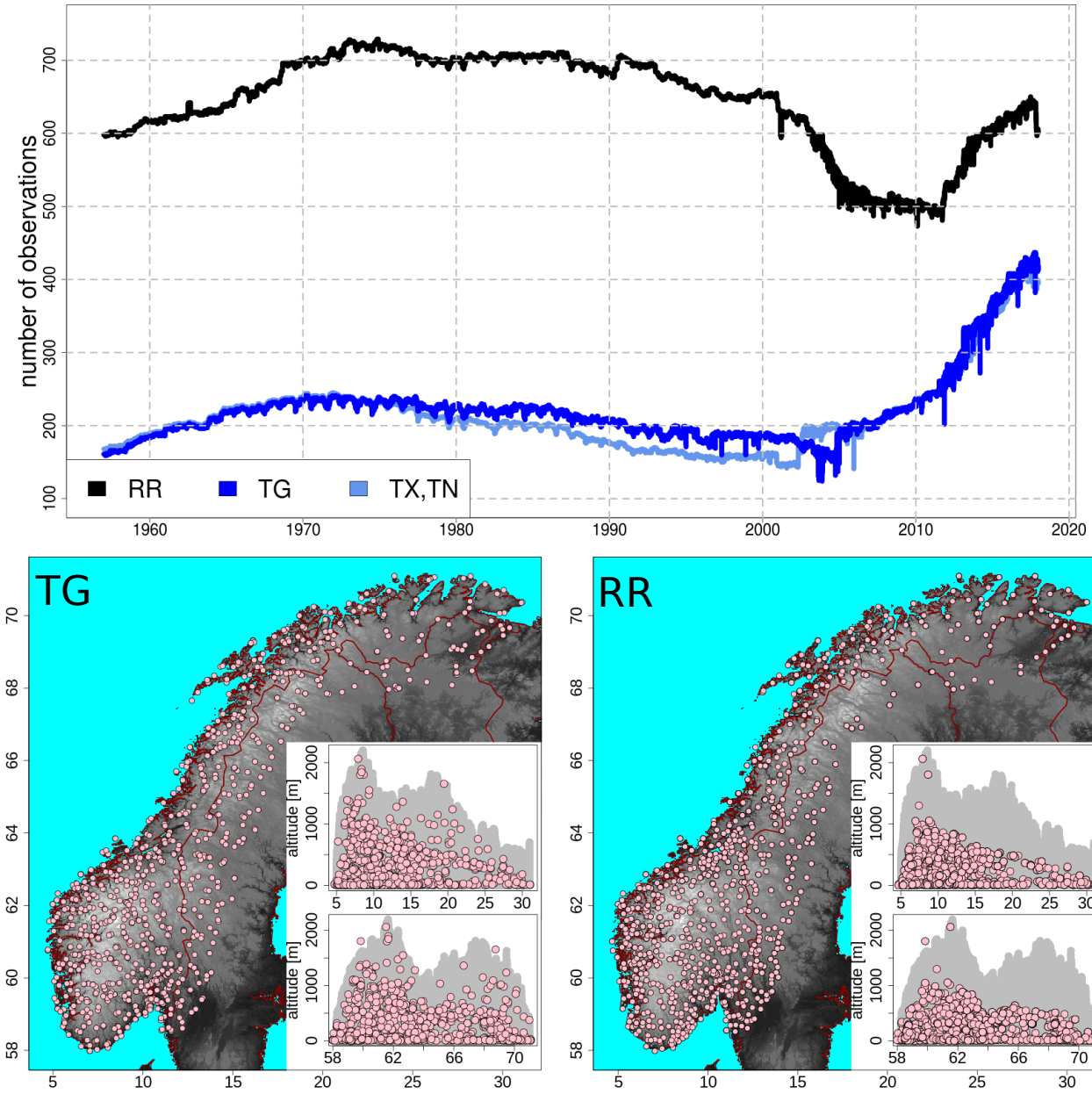

Figure 1. The observational network for the four variables: RR, TG, TX and TN. The top panel shows the time series for the number of available observations over the Norwegian mainland. [..[10]]The bottom panels [..[11]]show the observational networks for TG (left) and RR (right)[..[12]]. TX and TN are not shown because they are similar to TG[..[13]]. The pink dots [..[14]]mark station locations with more than 1 year of [..[15]]data. [..[16]]In the bottom panels, the geographic coordinate system is used [..[17]]and the [..[18]]maps show the domain with topographic information derived from a high-resolution digital elevation model (DEM). For each of the two bottom panels, the two inset graphs show altitude above mean sea level as a function of latitude (top graph) and longitude (bottom graph). In each inset graph, the gray area shows the altitude of the terrain at gridpoints, while the pink dots are the altitudes of stations.

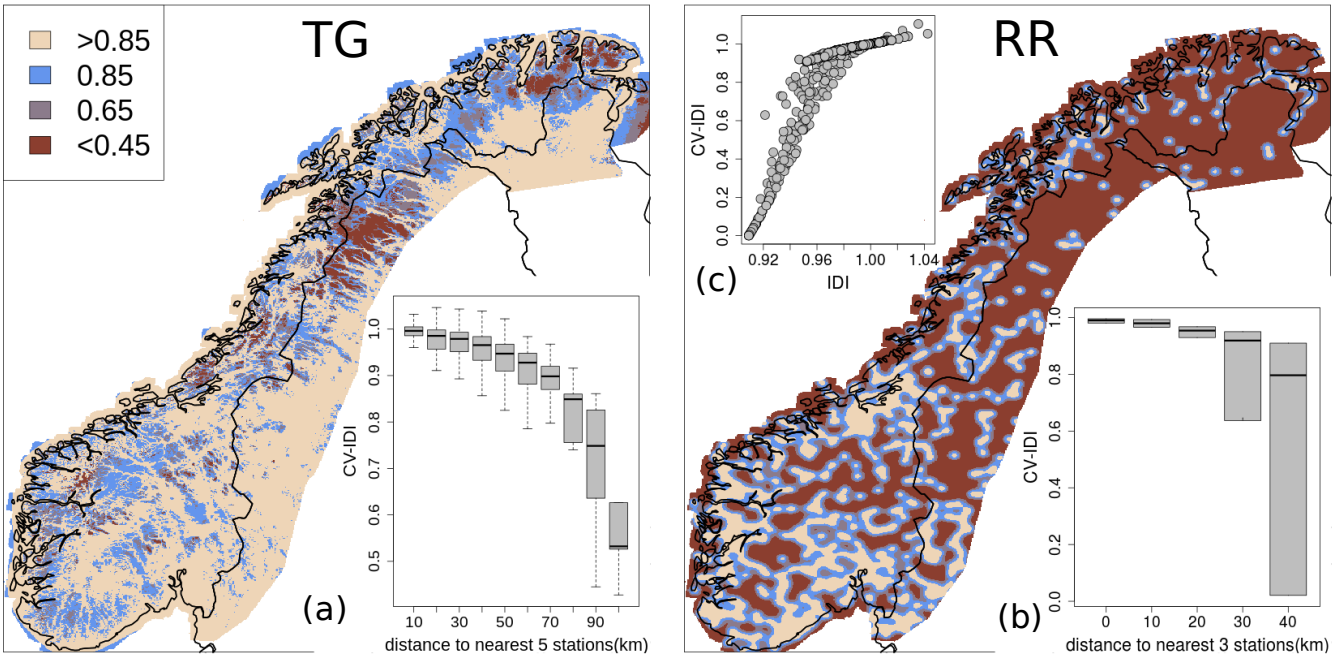

Figure 2. A representation of the observational network useful for spatial analysis of[..[19]]: TG (left) and RR (right). As for Fig.

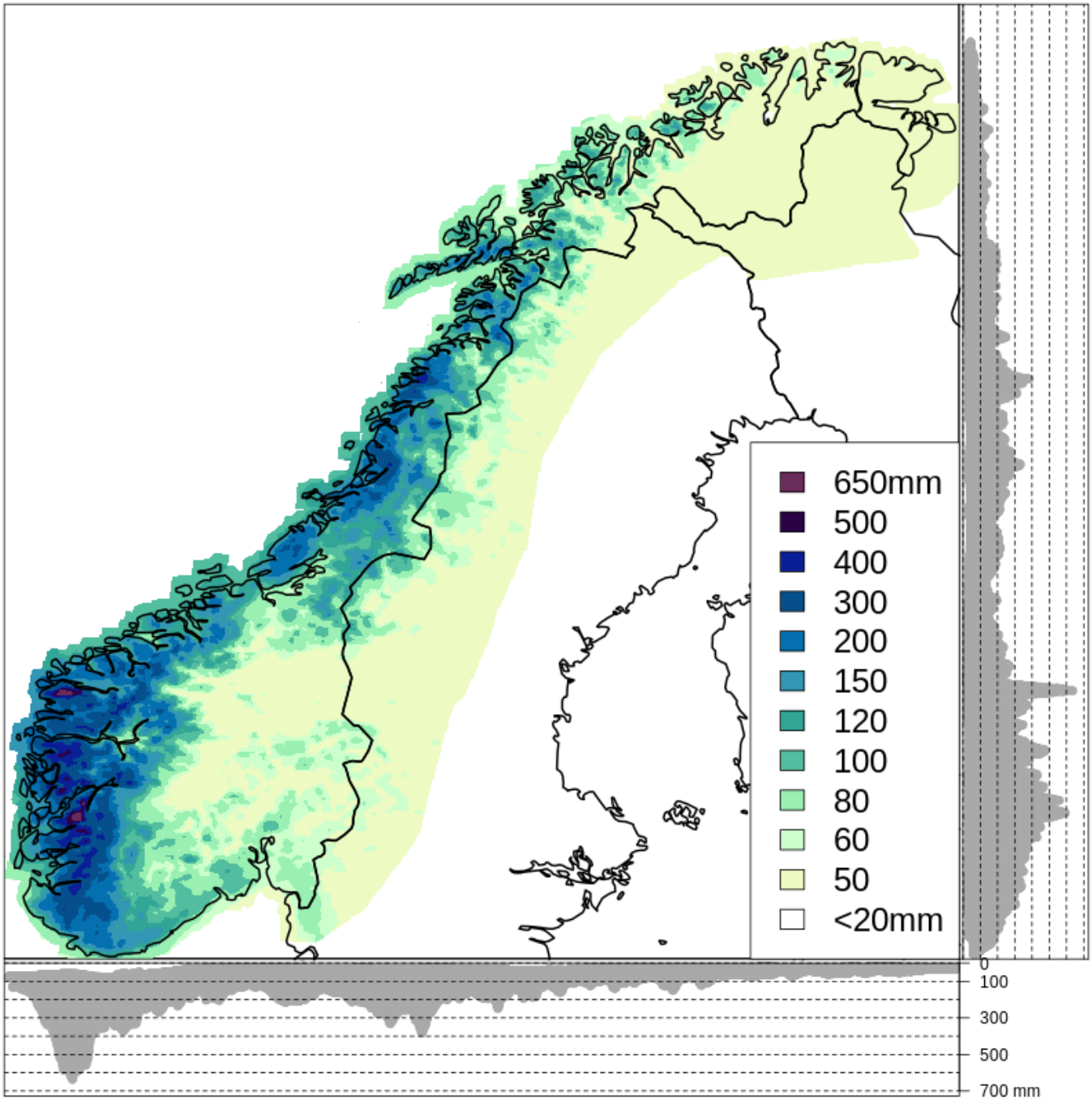

Figure 3. Precipitation reference field for October, that is $\mathbf{x}^{\mathrm{ref}}$ in Eq. (, used for the spatial analysis of RR for the day 1998-10-24 (Sec. . The lateral and bottom panels in both graphs show the projection of the [..[20]]reference precipitation values at gridpoints on the y- and the x- axis, respectively.

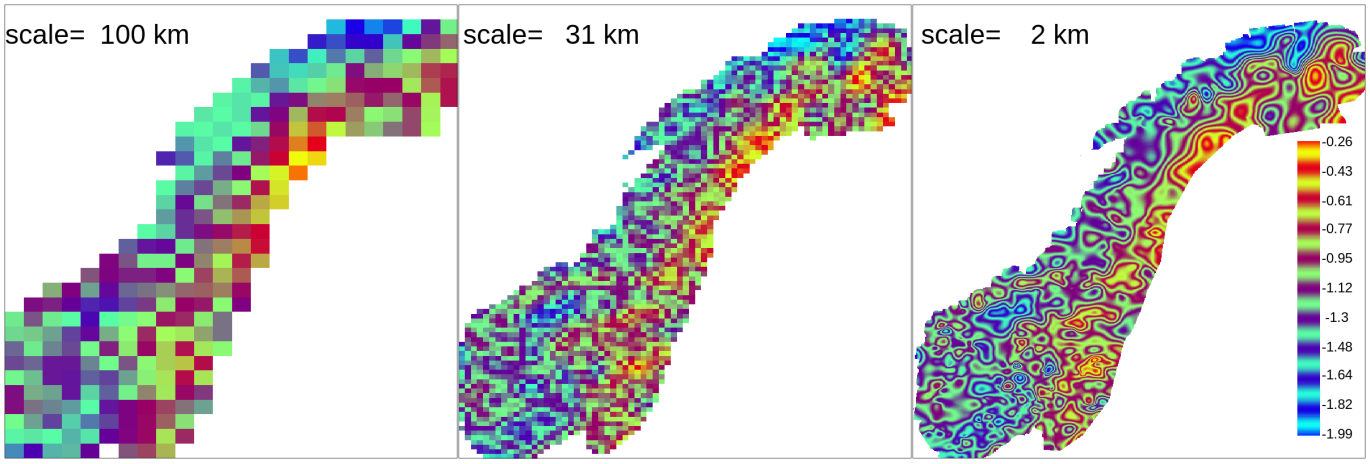

Figure 4. 1998-10-24 RR. Statistical interpolation of relative anomalies (dimensionless units) over different spatial length scales with the scheme reported in Eqs. (- (. The [..[21]]interpolation loops over a sequence of 91 decreasing spatial scales: 100 km is the seventeenth; 31 km is the sixty-ninth; 2 km is the ninety-first. The fields shown are three different $\overset{\alpha}{\mathbf{x}}^{a}$ (Eq. () for: $\alpha = 100$ km, $\alpha = 31$ km and $\alpha = 2$ km. In each of the the three cases, the interpolation is performed over a regular grid with the resolution of the integer value nearest to $\alpha/2$, that is: 50 km, 15 km and 1 km. The colour scale highlights the details in the field and it is the same for the three maps.

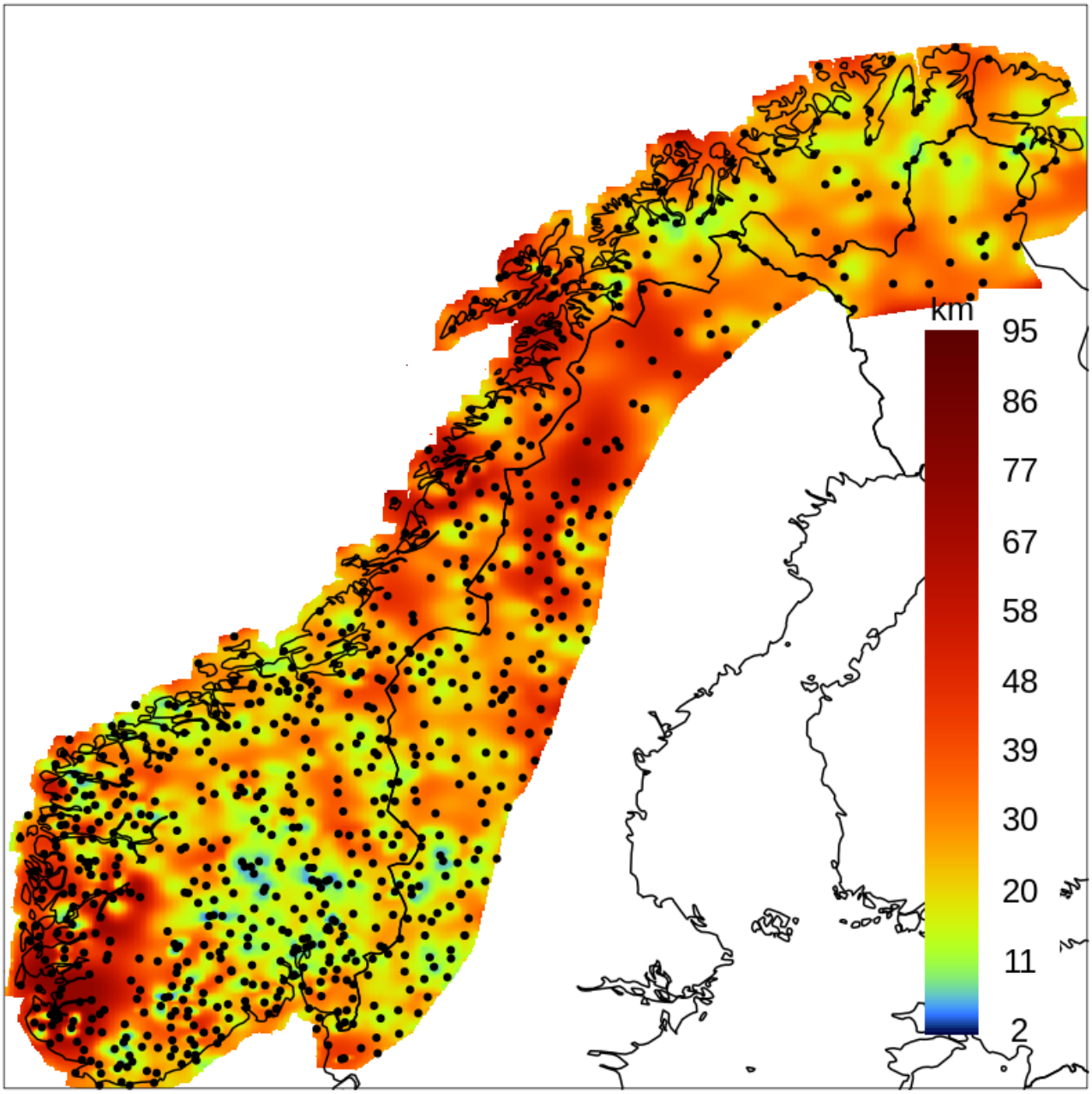

Figure 5. 1998-10-24 RR. [..[22]]"Critical" scale (Sec. [..[23]]
, values are in km) for the statistical interpolation scheme reported in Eqs. (- (given the observational network used (black dots mark the station locations). The critical scale varies for each gridpoint. For the [..[24]]ith gridpoint, the critical scale is the spatial scale α where the last significant variation of the interpolated [..[25]]relative anomaly $\overset{\alpha}{\mathbf{x}}{}^{a}{}_{i}$ has occurred with respect to the value $\overset{\beta}{\mathbf{x}}{}^{a}{}_{i}$ (or equivalently $\overset{\alpha}{\mathbf{x}}{}^{b}{}_{i}$) obtained for the immediately preceding scale β. A variation is considered significant when it is larger than 0.01 (dimensionless units) or 1%. The [..[26]]largest values of the [..[27]]critical scale may indicate either a data-sparse region or a region where stratiform precipitation is occurring. On the other hand, the smallest values occur in data-dense regions and they indicate regions where the field is highly variable over short distances (e.g., thunderstorms).

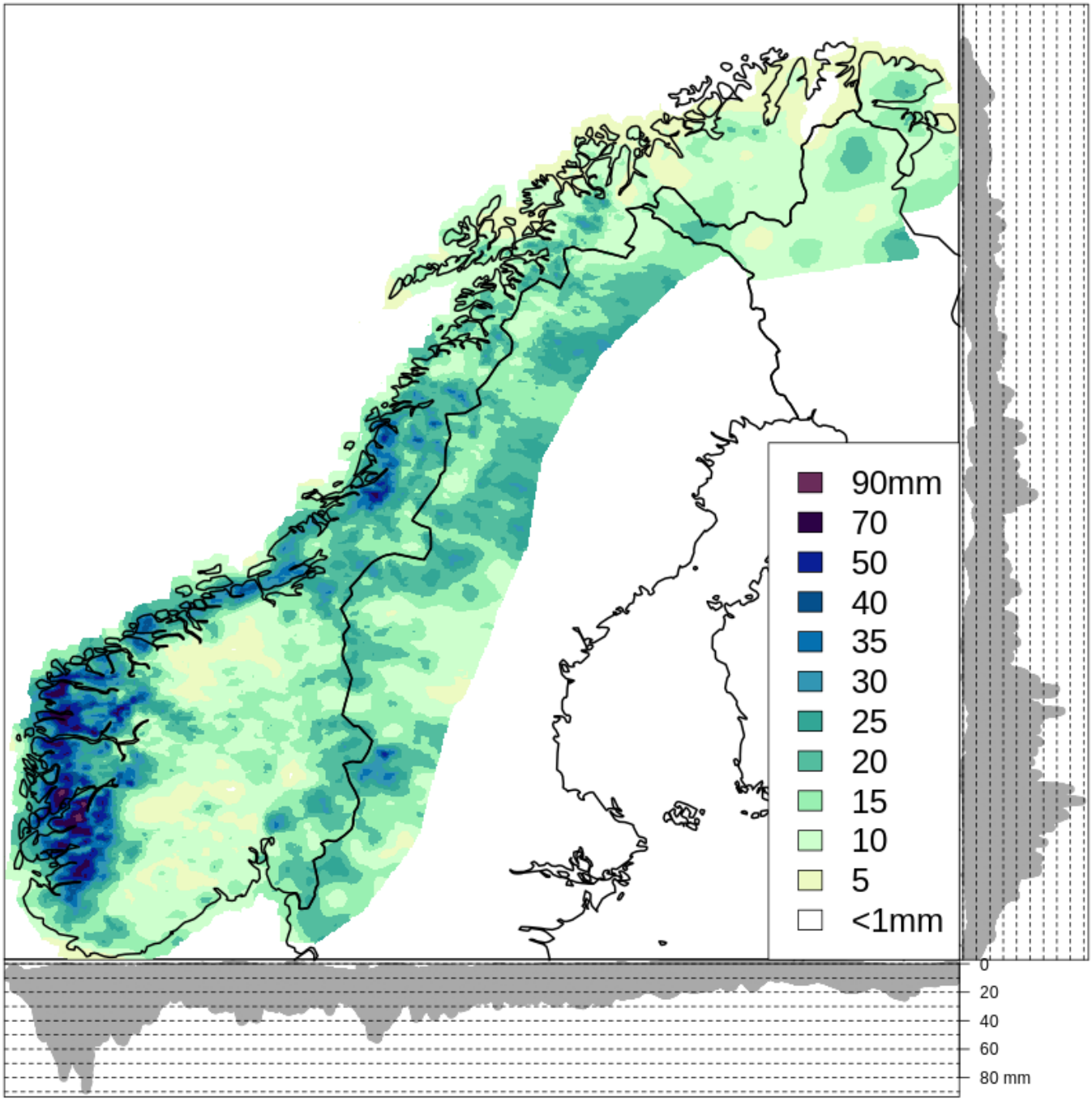

Figure 6. 1998-10-24, RR analysis field $\mathbf{x}^a$ of Eq. (. The lateral and bottom panels in both graphs show the projection of the differences on the y- and the x- axis, respectively.

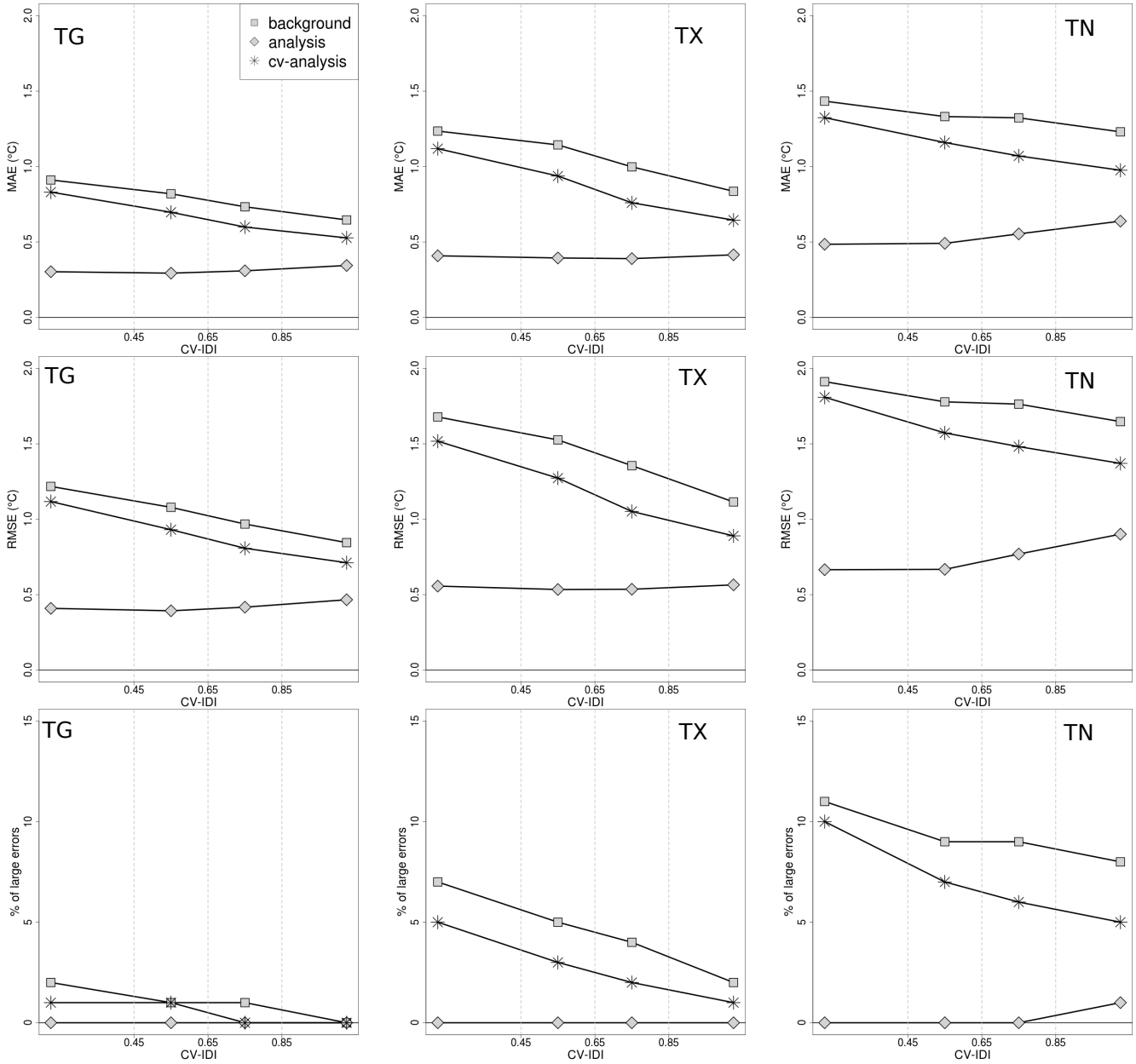

Figure 7. TG, TX and TN, verification scores as a function of CV-IDI [..[28]]for the summer seasons (June-July-August) [..[29]]of the 61-year time period 1957-2017. [..[30]]With reference to the definitions introduced in Sec.

scores: for the analysis are based on the analysis residuals; for the CV-analysis on the CV-analysis residuals; for the background on the innovation. On the top row, the mean absolute error (MAE). In the middle, the root mean square error (RMSE). On the bottom row, the percentage of large errors. A large error is defined as the absolute value of innovation or residual larger than 3°C.

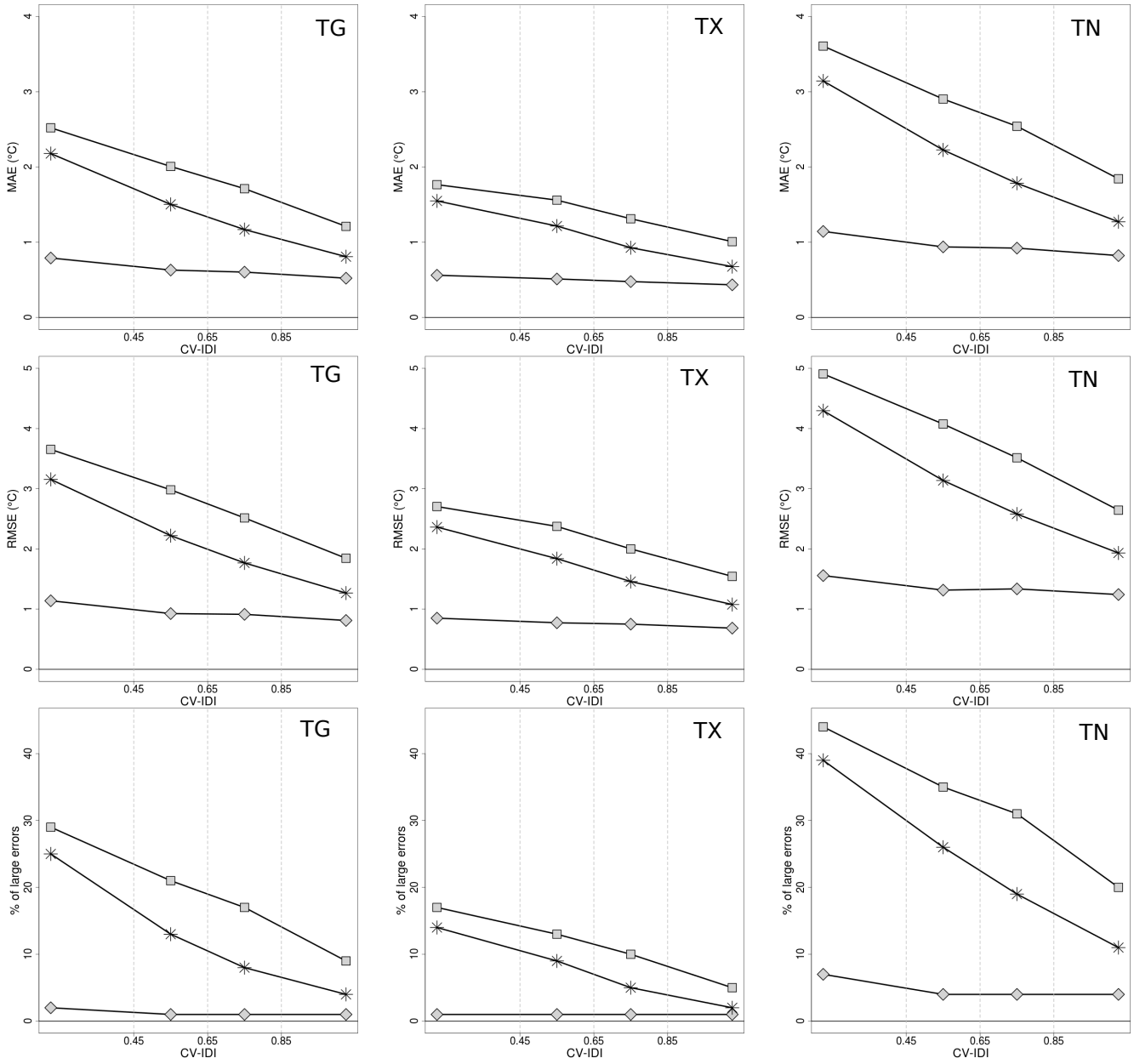

Figure 8. TG, TX and TN, verification scores as a function of CV-IDI [..[31]]for the winter seasons (December-January-February) [..[32]]of the 61-year time period 1957-2017. See Fig.

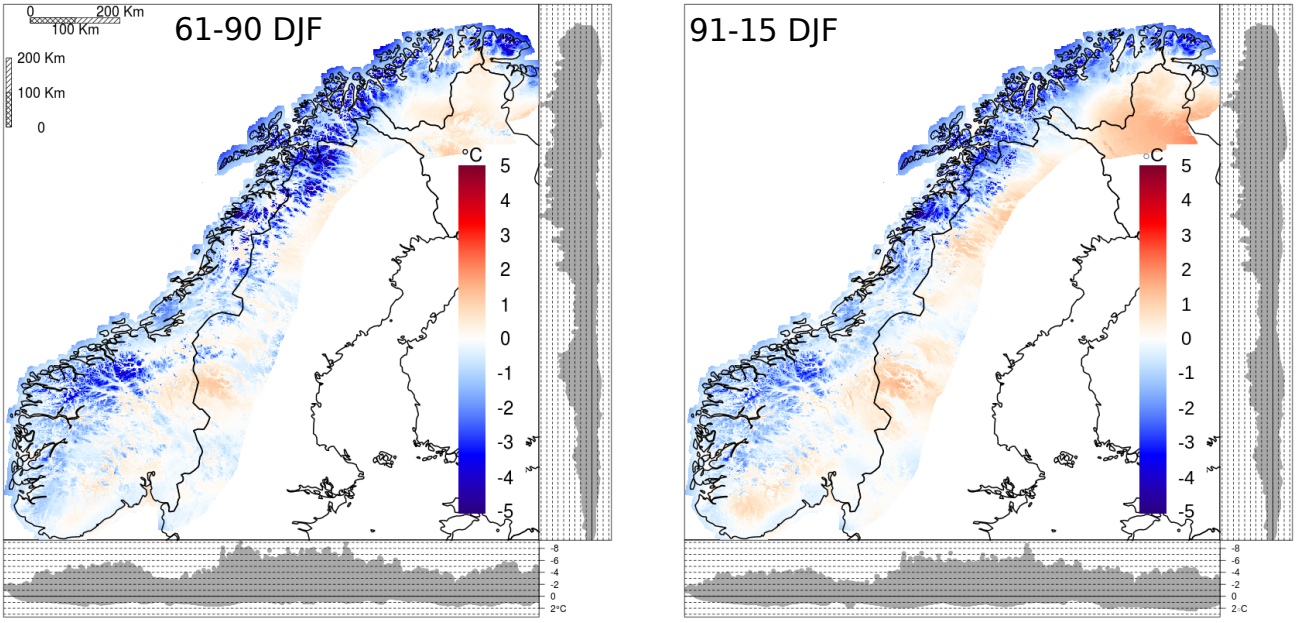

Figure 9. [..[33]]TG, mean difference between seNorge_2018 and seNorge2 [..[34]]daily analysis [..[35]]during winter (December-January-February). On the left panel, the 30-year period 1961-1990 is considered. On the right, the mean is based on the 25-year period 1991-2015. The lateral and bottom panels in both graphs show the projection of the [..[36]]values at gridpoints on the y- and the x- axis, respectively.

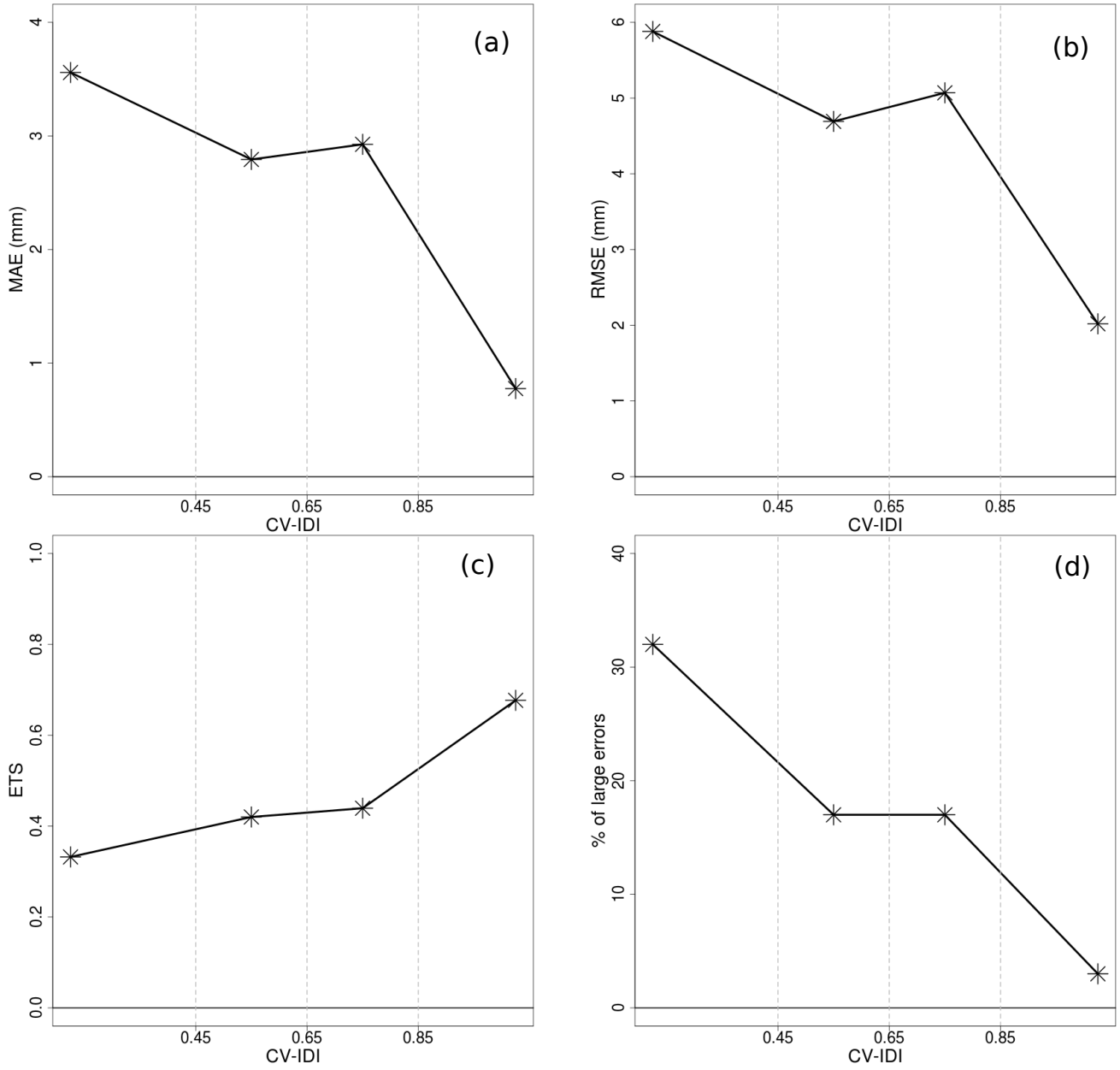

Figure 10. RR, CV-analysis verification scores as a function of CV-IDI [..[37]]for the 61-year time period 1957-2017. The terminology used is introduced in Sec.

Panel a, Mean Absolute Error (MAE) considering only observations greater than 1 mm/day. Panel b, Root-Mean-Squared Error (RMSE) considering only observations greater than 1 mm/day. Panel c, Equitable Threat Score (ETS) with threshold equals to 1 mm/day. Panel d, Percentage of large errors in case of intense precipitation[..[38]]. [..[39]]Intense precipitation is defined as an observed value greater than 10 mm/day[..[40]]. A large error is defined as the absolute value of a CV-analysis residual larger than 50% of the observed value.

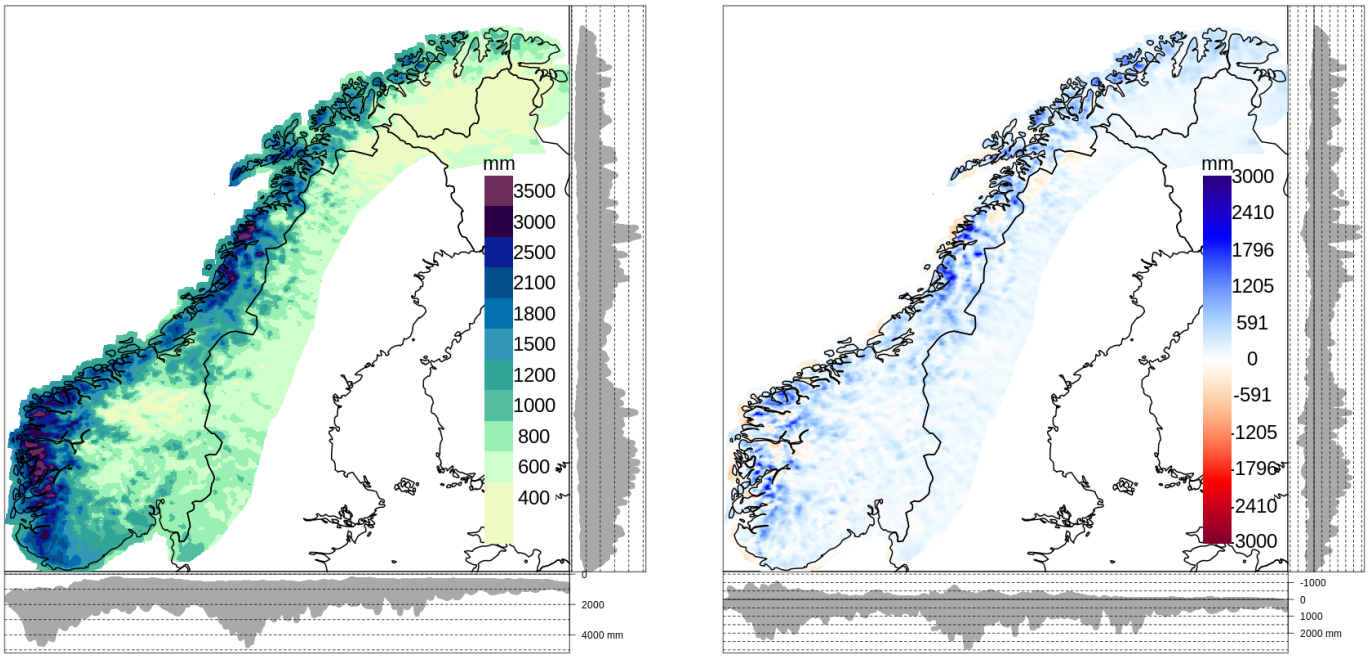

Figure 11. [..[41]]Annual total precipitation as derived by summing RR. On the left, the mean annual total precipitation based on the 61-year period 1957-2017: the lower precipitation class includes values smaller than 400 mm; the upper precipitation class values between 3500 mm and 4700 mm. On the right, mean annual total precipitation difference between seNorge_2018 and seNorge2 based on the 51-year period 1957-2015. On each graph, the lateral and bottom panels show the projection of the [..[42]]values at gridpoints on the y- and the x- axis, respectively.

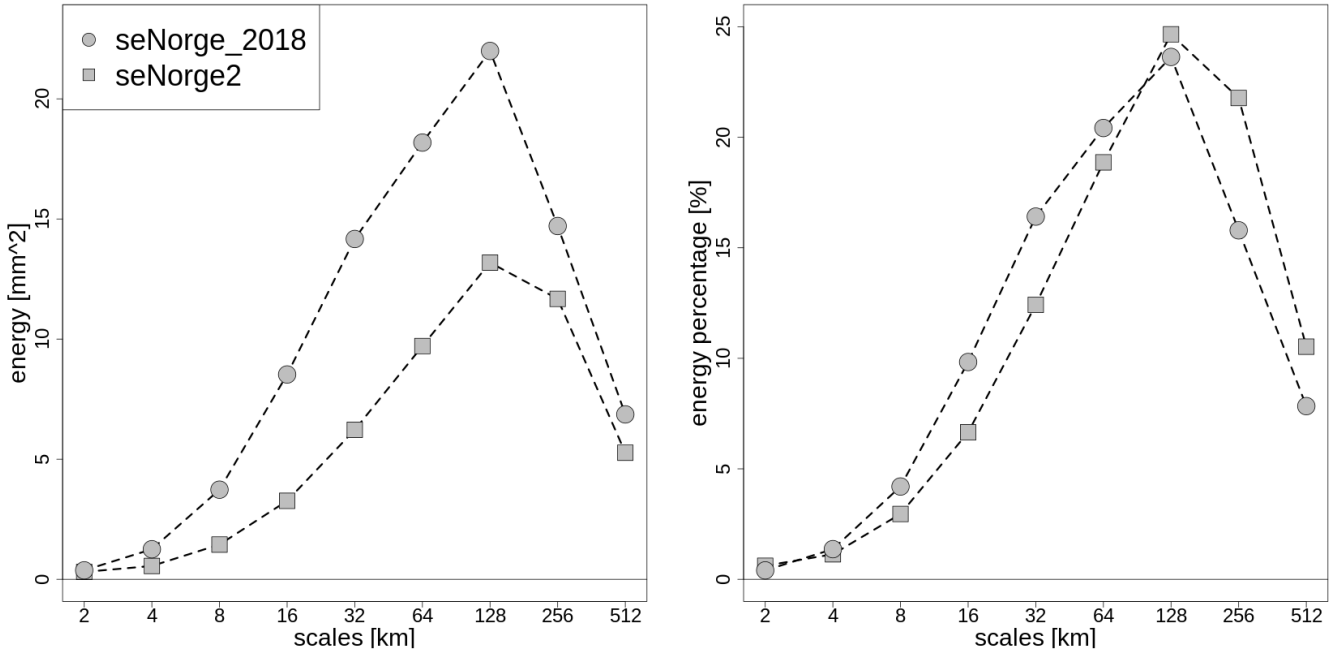

Figure 12. Scale decomposition of precipitation energy based on 2D discrete Haar wavelet transformation (Sec.

. On the left, the averaged energy as a function of the spatial scale for seNorge_2018 and seNorge2. On the right, the averaged percentage of [..[43]]energy as a function of the spatial scale for the same datasets. The statistics is based on the 25% of cases with the [..[44]]highest values of averaged precipitation over the domain.

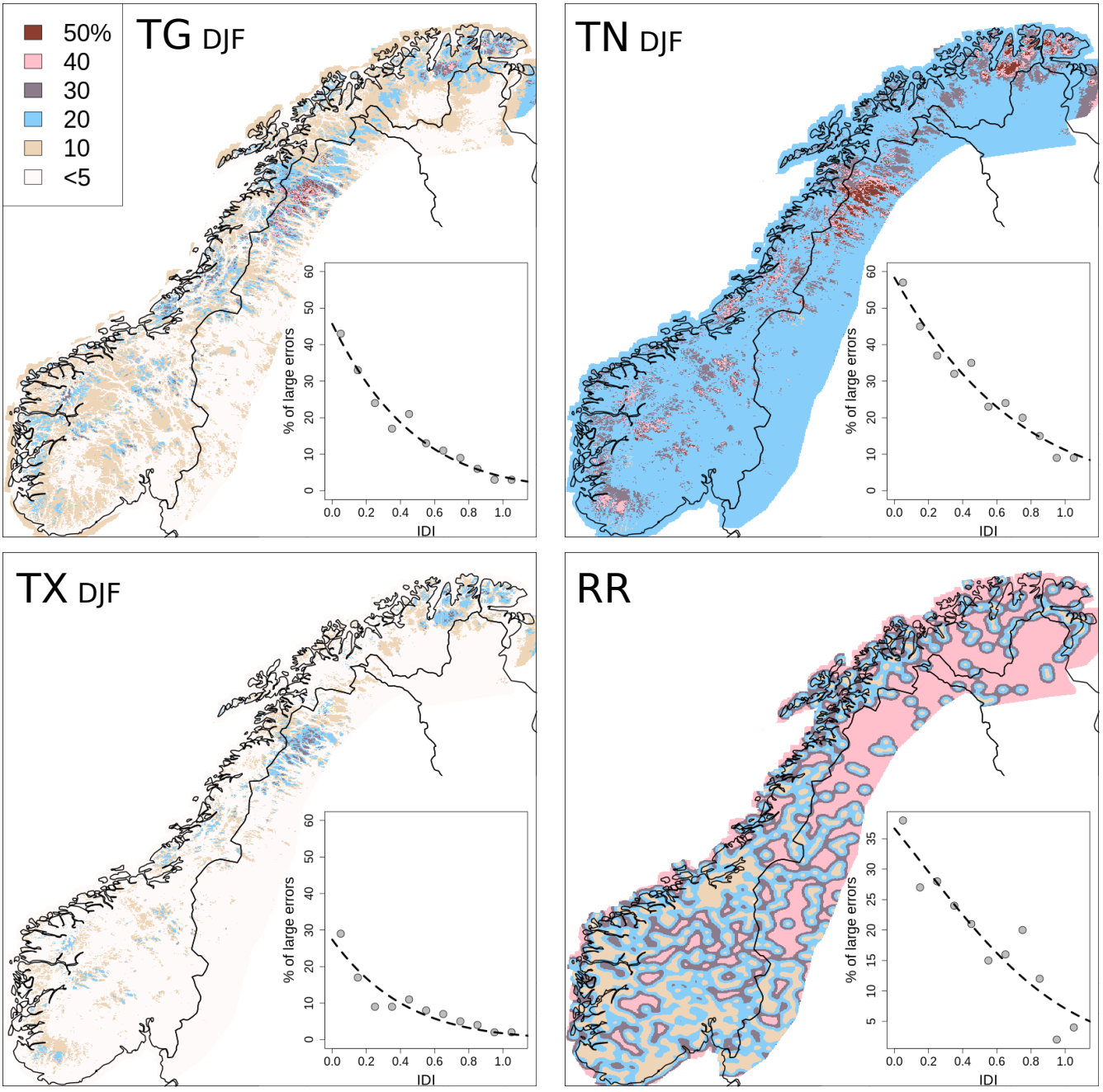

Figure 13. Expected [..[45]]percentages of large errors on the grid (dimensionless units) based on the summary statistics of the analyses and the spatial distribution of stations of the observational network. The colour scale is the same for all the maps. Wintertime (DJF) temperatures are considered, large errors are defined as deviations between analysis and unknown truth larger than 3°C. All precipitation data has been considered, large errors are deviations between analysis and unknown truth larger than 50% of the analysis value when the analysis value is greater than 10 mm/day. The insets show the relation between IDI and percentage of large errors: the dots correspond to the percentage of large errors observed at station locations (on the x-axis, CV-IDI instead of IDI); the dashed lines are the best-fit [..[46]]functions used to infer the expected percentage of large errors at gridpoints.

Table 1. TG annual statistics: "n" is the average number of stations; "d" (km) is the average distance between a station and its nearest third station; D^h (km), D^z (m), σ_b^2 ($(^\circ\mathrm{C})^2$) and σ_o^2 ($(^\circ\mathrm{C})^2$) are the spatial interpolation parameters defined in Sec.
optimal values [..[47]]of the [..[48]]interpolation parameters are obtained by imposing the constraint $\sigma_o^2/\sigma_b^2 = 0.5$ and considering the 1-year statistics of the innovation (observation minus background, Sec.

.

year	n	d	D^h	D^z	σ_b^2	σ_o^2
1960	398	55	60	206	2.24	1.12
1970	669	42	45	217	1.86	0.93
1980	639	42	58	201	2.45	1.22
1990	600	44	57	202	1.33	0.66
2000	627	44	55	206	1.28	0.64
2010	639	45	52	206	2.45	1.23

Table 2. TX annual statistics[..[49]]. See Tab.

year	n	d	D^h	D^z	σ_b^2	σ_o^2
1960	395	55	56	207	2.09	1.05
1970	669	42	57	201	1.67	0.84
1980	616	45	37	216	2.09	1.05
1990	563	47	55	206	1.40	0.70
2000	596	46	56	210	1.32	0.66
2010	638	45	57	206	2.09	1.04

Table 3. TN annual statistics[..[50]]. See Tab.

year	n	d	D^h	D^z	σ_b^2	σ_o^2
1960	396	55	50	217	4.42	2.21
1970	670	42	53	222	3.80	1.90
1980	615	45	62	211	4.58	2.29
1990	560	47	52	210	2.88	1.44
2000	596	46	51	210	2.99	1.49
2010	637	45	64	212	4.70	2.35